Pharmaceutical Research, Vol. 24, No. 7, July 2007 (© 2007)
DOI: 10.1007/s11095-007-9286-4

Research Paper

Coating Formulations for Microneedles

Harvinder S. Gill[1] and Mark R. Prausnitz[1,2,3]

Received December 16, 2006; accepted February 27, 2007; published online March 24, 2007

Purpose. To develop a rational basis for designing coating solution formulations for uniform and thick coatings on microneedles and to identify coating strategies to form composite coatings, deliver liquid formulations, and control the mass deposited on microneedles.
Materials and Methods. Microneedles were fabricated using laser-cutting and then dip-coated using different aqueous, organic solvent-based or molten liquid formulations. The mass of riboflavin (vitamin B_2) coated onto microneedles was determined as a function of coating and microneedle parameters. Coated microneedles were also inserted into porcine cadaver skin to assess delivery efficacy.
Results. Sharp-tipped microneedles, including pocketed microneedles, were fabricated. Excipients that reduced coating solution surface tension improved coating uniformity, while excipients that increased solution viscosity improved coating thickness. Evaluation of more than 20 different coating formulations using FDA approved excipients showed that hydrophilic and hydrophobic molecules could be uniformly coated onto microneedles. Model proteins were also uniformly coated on microneedles using the formulations identified in the study. Pocketed microneedles were selectively filled with solid or liquid formulations to deliver difficult-to-coat substances, and composite drug layers were formed for different release profiles. The mass of riboflavin coated onto microneedles increased with its concentration in the coating solution and the number of coating dips and microneedles in the array. Coatings rapidly dissolved in the skin without wiping off on the skin surface.
Conclusions. Microneedles and coating formulations can be designed to have a range of different properties to address different drug delivery scenarios.

KEY WORDS: coating formulations; dip-coating method; microfabricated microneedles; protein coatings; transdermal drug delivery.

INTRODUCTION

Conventional transdermal delivery of drugs is limited to small, lipophilic and potent molecules (1). As an alternative approach, microneedles provide a minimally invasive method to create micron-scale pathways into the skin for delivery of small and large molecular weight compounds including proteins, in a manner expected to be safe, painless and cost-effective (2,3). Microneedles are individual needles or arrays of needles having micron dimensions. They can be fabricated using micromachining tools adapted from the microelectronics industry (4). Both solid and hollow microneedles have been used in different modes to increase skin permeability by orders of magnitude to deliver large molecular weight molecules and nanoparticles into the skin (5–7). *In vivo* delivery has been shown for small molecules (8,9); peptides, such as insulin (6,8, 10) and desmopressin (11); genetic material, including plasmid DNA (12) and oligonucleotides (13); and vaccines directed against hepatitis B (12) and anthrax (14).

An attractive method of transdermal delivery using microneedles involves the use of coated microneedles (15). This process involves coating a drug formulation onto solid microneedles and inserting them into the skin for subsequent dissolution of the drug within the skin. Coated microneedles have previously been shown to deliver peptides (11) and proteins (16) into the skin *in vivo*. Robust immune responses have also been generated in guinea pigs against an ovalbumin model antigen using this approach (17).

Although, coated microneedles have been used to deliver proteins and drugs into the skin, detailed studies of the coating process itself have not been published. Excipients are known to affect drug stability and activity (18), and therefore a single coating formulation may not be universally applicable to coat all therapeutic compounds and proteins. Therefore, it is desirable to identify a rational basis for designing coating formulations and different coating strategies, which can enable uniform coating of therapeutics with diverse physicochemical properties. To address this, we sought to study the effects of coating methods and formulations, and thereby provide a rational basis for designing microneedles and coating formulations for different applications. The micron length scales of microneedles impose special coating challenges to obtain uniform coatings and to obtain spatial control over the region of the microneedle to be coated. This is largely because the effects of surface tension, capillarity and

[1] Wallace H. Coulter Department of Biomedical Engineering at Georgia Tech and Emory University, Georgia Institute of Technology, 313 Ferst Drive, Atlanta, Georgia 30332-0535, USA.
[2] School of Chemical & Biomolecular Engineering Georgia Institute of Technology, 311 Ferst Drive, Atlanta, Georgia 30332-0100, USA.
[3] To whom correspondence should be addressed. (e-mail: prausnitz@gatech.edu)

viscous forces become more prominent at these small length scales. Therefore, in a companion study, we developed a novel micro-dip-coating process that applied uniform coatings with micron-scale control over the length of the microneedle shaft to be coated (15). Using this device we investigated the range of compounds and molecules that can be coated onto microneedles and found that small molecules, proteins, DNA, viruses and microparticles as large as 10 μm in diameter could be applied onto microneedles as uniform and stable coatings (15). Coatings were applied not only to the surface of microneedles, but could also be filled into 'pocket' cavities cut into the microneedles.

This study seeks to address the physical chemistry of coating formulations in greater detail to: (1) determine factors that affect coating uniformity and thickness, (2) develop composite drug coatings to expand the utility of coated microneedles, (3) deliver liquid formulations using solid microneedles, and (4) examine the effect of microneedle and coating parameters on the mass of drug coated onto microneedles. To attain these objectives, we varied the physical properties of the coating solution formulations to control the fluid mechanics of the dip-coating process and the thermodynamics of microneedle surface wetting.

The process of wetting a solid with a liquid under static conditions is described by the Young equation. According to this equation, the contact angle should be zero for the liquid to spread on the solid surface to form a uniform liquid film (19), which, upon drying, would provide a uniform solid coating on the solid substrate. In a coating process, however, the system is not at rest but in a dynamic state as the microneedle gets dipped into and out of the dipping solution and the gravity and local surface tension gradients cause micro-flows in the liquid film adhering to the microneedle surface. Therefore, the static contact angle is no longer an adequate measure of spreading, and the dynamic equilibrium depends upon: (1) the hydrodynamics of the system, (2) the physical properties of the coating solution and the solid substrate, and (3) the rate of evaporation of the solvent (19). Unfortunately, the complex physics of dynamic wetting is not fully understood, which makes theoretical predictions of coating uniformity and thicknesses difficult (19,20). Therefore, while an understanding of the physics of coating can serve as a guide, the control and optimization of microneedle coatings requires experimental study.

Based on the physics of dip-coating, it is recognized that the dip-coating process consists of two distinct steps generally occurring in sequence: (a) the dipping and withdrawal step, resulting in the formation of a liquid film on the solid substrate, and (b) the drying step, resulting in the conversion of the adherent liquid film into a solid coating (21). In the first step, the formation of the liquid film after dipping and withdrawal is fluid mechanically controlled, such that the thickness of the liquid film formed on the solid substrate depends on the withdrawal speed of the solid substrate and the physical properties of the coating solution, notably the surface tension and viscosity (21). A faster withdrawal speed of the solid substrate, a higher viscosity of the coating solution, and a lower surface tension of the coating solution tend to produce thicker liquid films. There correspondingly exists a critical speed of withdrawal for each coating solution-substrate combination, below which a liquid film does not form on the substrate because the hydrodynamic force of withdrawal is unable to overcome the forces of gravity and solution surface tension. If the substrate is withdrawn above the critical speed, an adherent liquid film is formed even from thermodynamically de-wetting liquids due to the hydrodynamic drag, which overcomes the opposing forces of surface tension and gravity. However, air entrainment in the liquid film at very high withdrawal speed prevents usage of systems with excessively high critical speed requirements (19,21).

In the second step involving drying of the adherent liquid film on the substrate, the fate of the entrained liquid film is determined by a complex interaction of the hydrodynamics of the entrained liquid film, the rate of solvent evaporation, and the tendency of the liquid film to attain its thermodynamic equilibrium on the solid surface (21,22). Thermodynamically, the deposited liquid film may completely wet the surface, which favors formation of a uniform coating, or, alternatively, may have a tendency to de-wet the surface via a surface tension-driven contraction. In this case, increasing the coating solution viscosity can significantly slow down the de-wetting process and provide the coating solution sufficient residence time on the solid surface to allow for solvent evaporation to form the solid film before de-wetting can occur (21). This kinetic effect, therefore, provides a means to coat devices with liquid formulations that thermodynamically favor de-wetting of the solid surface.

Guided by these physical principles, this study investigated the effect of coating solution surface tension and viscosity, and microneedle surface modification on (1) microneedle coating uniformity, (2) the mass of drug coated on microneedles, and (3) the ability to fill pockets in microneedles with coating solution. The coating solution surface tension was modulated by the addition of surfactants and by using non-aqueous solvents. The coating solution viscosity was also modified to increase the coating thickness in order to coat larger amounts of a model drug onto microneedles.

MATERIALS AND METHODS

Fabrication of Microneedles

Using methods described in detail previously (15), microneedle geometries were first drafted in AutoCAD software (Autodesk, Cupertino, CA, USA) and then cut into 75 μm thick stainless steel sheets (Trinity Brand Industries, SS 304; McMaster-Carr, Atlanta, GA, USA) using an infrared laser (Resonetics Maestro, Nashua, NH, USA). To form pockets in microneedles, the desired shapes, dimensions and locations of the pockets on the microneedle shaft were also drafted and then cut together with the microneedles. 'In-plane' microneedles were fabricated as one-dimensional rows of microneedles oriented parallel to their base substrate. 'Out-of-plane' microneedles were fabricated as two-dimensional arrays with microneedles bent perpendicularly out of the plane of their base substrate.

To deburr and clean microneedle edges and pockets, and to make the tips sharp, microneedles were electropolished in a solution containing glycerin, ortho-phosphoric acid (85%) and water in a ratio of 6:3:1 by volume (Fisher Chemicals,

Fair Lawn, NJ, USA) by applying 1.8 mA/mm^2 of current for 15 min. Microneedles were then washed under running water, dried using compressed air, and stored in air-tight containers until later use.

Micron-scale Dip-coating

Single microneedles, and arrays of multiple microneedles, were coated with molecules using a micron-scale dip-coating process developed previously (15). Briefly, a coating solution containing a model drug and, in most cases, a surfactant and a viscosity enhancer was prepared in an aqueous or organic solvent. Microneedles were then dipped into the coating solution held in a dip-coating device. Coatings were formed by dipping just once into the coating solution, unless otherwise specified. The withdrawal speed of microneedles from the coating solution was manually maintained at approximately 2 mm/s to produce solid films and at approximately 0.35 mm/s to fill the pockets with a liquid. The microneedles coated with solid films were allowed to air-dry for at least 24 h before use, whereas the pocketed microneedles filled with liquid were used immediately to minimize liquid evaporation.

Coating Solution Formulations

Aqueous coating solution formulations (w/v % unless otherwise specified) were prepared using DI water according to the following recipes: *Formulation A1*: 0.1% sulforhodamine (Molecular Probes, Eugene, OR, USA). *Formulation A2*: 1% carboxymethylcellulose sodium salt (CMC, low viscosity, USP grade, CarboMer, San Diego, CA, USA), 0.5% Lutrol F-68 NF (BASF, Mt. Olive, NJ, USA), 0.1% sulforhodamine. *Formulation A3*: 52% (w/w) sucrose (Fisher Chemicals), 0.2%(w/w) Tween 20 (Sigma, St. Louis, MO, USA), 0.1% sulforhodamine. *Formulation A4*: 0.5% hyaluronic acid (Sigma), 0.5% Lutrol F-68 NF, 0.1% sulforhodamine. *Formulation A5*: 0.5% xanthan gum (Sigma), 0.5% Lutrol F-68 NF, 0.1% sulforhodamine. *Formulation A6*: 1% sodium alginate (Sigma), 0.5% Lutrol F-68 NF, 0.1% sulforhodamine. *Formulation A7*: 5% polyvinylpyrrolidone (BASF), 0.5% Lutrol F-68 NF, 0.1% sulforhodamine. *Formulation A8*: 52% (w/w) sucrose, 0.5% Lutrol F-68 NF, 0.1% sulforhodamine. *Formulation A9*: 25% sucrose, 0.1% sulforhodamine. *Formulation A10*: 80% (v/v) glycerol, 20% (v/v) aqueous solution of 0.1% sulforhodamine. *Formulation A11*: 1% CMC, 0.5% Lutrol F-68 NF, 0.2% sodium fluorescein (Sigma). *Formulation A12*: 80% (v/v) glycerol, 20% (v/v) green food dye (Kroger, Atlanta, GA, USA). *Formulation A13*: 80% (v/v) glycerol, 20% (v/v) yellow food dye (Kroger). *Formulation A14*: 80% (v/v) glycerol, 20% (v/v) red food dye (Kroger).

Organic solvent coating solution formulations (w/v % unless otherwise specified) were prepared according to the following recipes: *Formulation O1*: 5% poly(lactic-co-glycolic acid) (PLGA, Absorbable Polymer International, Pelham, AL, USA) in acetonitrile (Fisher Chemicals). *Formulation O2*: 5% polyvinylpyrrolidone, 0.1% curcumin (Fisher Chemicals) in ethanol (Fisher Chemicals). *Formulation O3*: 5% PLGA, 0.03% sulforhodamine in acetonitrile.

Coating Solution Viscosity and Contact Angle Measurement

Viscosity of the aqueous coating solution containing CMC and sucrose was measured using an Ubbelohde type viscometer (viscometer no. 200-c21, Cannon Instrument Company, State College, PA, USA). Static advancing contact angles of the coating formulations containing various excipients were measured on electropolished stainless steel using a VCA 2500 XE contact angle system (AST Products, Billerica, MA, USA). Both the viscosity and the contact angles were measured at room temperature with a sample size of at least $n = 5$ for each solution.

Effect of Coating Solution Surface Tension and Viscosity

To study the significance of surfactants and viscosity enhancers in producing uniform coatings on microneedles, single microneedles ($n = 3$) were dipped in formulations A1, A2 and A3. Aqueous solutions of individual constituents of formulations A2 and A3 with 0.1% sulforhodamine were also used to evaluate their relative and synergistic effects. Further, to assess the ability of different viscosity enhancers to produce uniform coatings using Lutrol F-68 NF as the surfactant, single microneedles ($n = 3$) were dipped in formulations A4, A5, A6, A7 and A8. Dipped microneedles were air-dried for 24 h and examined by fluorescence microscopy using an Olympus IX70 fluorescence microscope (Olympus America, Center Valley, PA, USA) with a CCD camera (RT Slider, Diagnostic Instruments, Sterling Heights, MI, USA) to assess coating uniformity.

Microneedle Surface Modification

To enable coating of microneedles without the use of excipients in the coating solution, we modified the stainless steel surface properties by depositing silicon dioxide or PLGA. Silicon dioxide was deposited using a vapor deposition method (PlasmaTherm PECVD, Plasma-Therm, St. Petersburg, FL, USA), while PLGA was deposited by dipping the microneedles in formulation O1. Surface-modified microneedles were then dipped into formulation A1, dried, and examined by fluorescence microscopy to assess coating uniformity.

Coatings Involving Hydrophobic Molecules, Molten Coating Solutions and Pocketed Microneedles

To coat hydrophobic molecules, single microneedles ($n = 3$) were dip-coated using formulations O2 or O3. Microneedles dipped in formulation O2 were immersed in water for 15 s and checked for loss of coating from the microneedle surface by fluorescence microscopy. To apply coatings of essentially 100% drug, single microneedles with or without rectangular pockets (400 μm long × 50 μm wide) were dipped in molten liquid solutions of lidocaine (Sigma) at 100°C or polyethylene glycol (MW 1500, Fisher Chemicals) at 45°C, each containing up to 0.01% (w/v %) sulforhodamine. A hot plate was used as the heat source.

To apply coatings into microneedle pockets, single microneedles ($n = 3$) with a rectangular pocket 400 μm long and 50 μm wide were dipped in formulation A2, A9 or A10. To coat both the microneedle surface and the pockets using formulation A2, a total of six dips each separated by 15 s were used. Multiple dips separated by drying intervals enabled filling the pockets with more material as compared to just a single dip. However, for formulations A9 and A10, single dips were used to fill just the pockets. For formulation A9, single dips prevented patchy coatings on the surface that can result from repeated dips and microneedle surface irregularities. For formulation A10, a single dip was sufficient to fill just the pockets, because the coating remained as a liquid phase. After each of these coating procedures, microneedles were air dried for at least 24 h and examined by fluorescence microscopy to assess coating uniformity. However, the liquid-filled pocketed microneedles were used immediately for imaging or insertion into porcine cadaver skin to minimize liquid evaporation.

Composite Coatings

Single microneedles with or without pockets were sequentially dipped in different formulations to produce composite coatings of multiple molecules. Four different schemes were evaluated. (1) Pocketed microneedles with three circular pockets (90 μm diameter each) were sequentially dipped into different formulations to fill each pocket with a separate solution. This was achieved by first dipping all three microneedle pockets into formulation A12 and then sequentially dipping them into DI water, formulation A13, DI water and formulation A14. At each DI water wash step, the length of microneedle immersed into the wash water and all subsequent dip solutions was sequentially decreased by one pocket length to retain the formulation filled in the pocket from the previous dip, but cleaning the other pocket(s). (2) Non-pocketed microneedles were dipped into formulation O3 (six dips) and then into formulation A11 (six dips). (3) Non-pocketed microneedles were sequentially dipped into formulation A2, O1 and A11. (4) Microneedles with a rectangular pocket (400×50 μm) were dipped sequentially into formulations A9, O1 and A11. Between sequential dips and after completion of composite coatings, microneedles were air dried and imaged by fluorescence microscopy.

Protein Coatings

To assess the ability of optimized formulations to coat proteins, fluorescein isothiocyanate-labeled, (1) insulin derived from bovine pancreas (MW = 6 kDa, Sigma) and (2) bovine serum albumin (BSA) (MW = 66 kDa, Sigma) were coated onto microneedles ($n = 3$). Insulin (0.075% w/v) and BSA (0.15% w/v) were each coated onto single microneedles using excipients of formulations A2, A4 and A6. Microneedles were then air dried and imaged by fluorescence microscopy.

Determination of Mass in Coatings

To modulate the mass of material coated onto microneedles, coating parameters and microneedle parameters were investigated. The coating parameters that were studied included, (1) the concentration of a model drug in the coating solution and (2) the number of dips during coating, and the microneedle parameters that were investigated included, (1) the number of microneedles in the array and (2) the ability to selectively fill the microneedle pockets. Riboflavin (vitamin B_2, riboflavin-5′-phosphate sodium salt dihydrate, Fisher Chemicals) was used as the model drug in the coating formulations. In-plane rows of microneedles were dipped into a solution containing 1% sodium salt of CMC, 0.5% Lutrol F-68 NF and a range of riboflavin concentrations. For the study of coating parameter (1), riboflavin was used at 0.01, 0.1, 1, 2, 3 and 4% concentrations ($n = 5$ rows for each condition) with six dips at 15 s intervals between dips. For coating parameter (2), a 3% riboflavin concentration was used with 1, 3, 6, 12 or 24 dips at 15 s intervals between dips ($n = 5$ rows for each condition). To study microneedle parameter (1), a 3% riboflavin solution was used with out-of-plane arrays having 5 or 50 needles ($n = 3$ arrays for each condition) with six dips at 15 s intervals between dips. To investigate microneedle parameter (2), i.e. the ability of pocketed microneedles to carry the model drug exclusively within the pockets and without coating the surfaces, in-plane rows with five microneedles each having a rectangular pocket (400×50 μm) were dipped into an aqueous formulation containing 1 or 3% riboflavin and 25% sucrose with six dips at 15 s intervals between dips. All coated microneedles were allowed to dry for at least 24 h and imaged by brightfield microscopy using an Olympus SZX12 stereo microscope (Olympus America) with a CCD camera (Leica DC 300, Leica Microsystems, Bannockburn, IL, USA). The mass of riboflavin in the coatings was determined by dissolving the coatings off the microneedles by immersing in DI water and vortexing for 1 min, and then measuring riboflavin concentration by calibration fluorescence spectroscopy (SpectraMax Gemini, Molecular Devices, Sunnyvale, CA, USA; excitation = 450 nm, emission = 534 nm). The mass of riboflavin in the coatings was then calculated by multiplying the riboflavin concentration by the volume of DI water used to dissolve the coatings (typically 1 ml).

Microneedle Delivery into Skin *In Vitro*

Single, non-pocketed microneedles coated with formulation A2 ($n = 3$) and single, pocketed (rectangular pocket—400×50 μm) microneedles coated with formulation A10 ($n = 3$) were each manually inserted into abdominal porcine cadaver skin for 20 s and then removed. Microneedle insertion speed was manually maintained at 0.5–1 mm/s or 1–2 cm/s for microneedles coated with formulation A2 and A10, respectively. After removing the microneedles, the skin surface was examined by brightfield microscopy for coating residue. The skin was then examined histologically to assess the extent of delivery of microneedle coatings into the skin. The use of porcine cadaver skin has been approved by the Georgia Institute of Technology Institutional Animal Care and Use Committee (IACUC).

Microneedle Penetration into Skin of Human Subjects

For *in vivo* analysis, out-of-plane arrays of non-coated microneedles were assembled into adhesive patches (15),

ethylene oxide sterilized, and manually applied to the volar forearms of human subjects ($n = 3$). After removing the microneedle patch, gentian violet (2% solution, Humco, Texarkana, TX, USA) was applied to the treated site for 1 min and then wiped away using isopropanol swabs. Gentian violet selectively stained the sites of skin perforation, which identified the sites of microneedle penetration. The use of human subjects has been approved by the Georgia Institute of Technology Institutional Review Board (IRB).

RESULTS AND DISCUSSION

Microneedles for Coating and Insertion

Stainless steel microneedles with appropriate mechanical properties, sharp tips and clean edges were prepared in different configurations for dip-coating. Microneedles were fabricated as single microneedles without pockets (Fig. 1a), single microneedles with three circular pockets each 90 μm in diameter (Fig. 1b), single microneedles with a single rectangular pocket measuring 400 by 50 μm (Fig. 1c), in-plane microneedle rows each containing five microneedles (Fig. 1d) and out-of-plane microneedle arrays each with 50 microneedles (Fig. 1e). All needles were 700 μm in length, 160 μm in width and 50 μm in thickness. In-plane rows each with five, rectangular pocketed (400 by 50 μm) microneedles were also fabricated (image not shown).

Uniform Coatings with Spatial Control

For dose reliability, it is critical to consistently apply uniform coatings just to the microneedle shafts without contaminating the substrate. Using custom-designed dip-coating devices, microneedles of different configurations including single microneedles, in-plane rows of microneedles and out-of-plane microneedles, were uniformly coated with spatial control over the microneedle length being coated. A representative example of a riboflavin-coated, out-of-plane microneedle array containing 50 microneedles is shown in Fig. 2a and a representative magnified view of a single microneedle from the coated array is shown in Fig. 2b. The properties of coating solution excipients required to obtain uniform coatings are quantitatively assessed below.

Effect of Coating Solution Surface Tension and Viscosity

Dose reproducibility and a high drug loading into microneedle coatings are critical for pharmaceutical drug and vaccine delivery applications of coated microneedles. This requires precision deposition of uniform and thick coatings onto microneedle shafts. Control over physical properties and kinetic parameters that affect the thermodynamics and hydrodynamics of dip-coating are expected to result in uniform and thick coatings. The two important physical properties of the dipping formulation that are known to influence the thermodynamics and hydrodynamics of dip-coating are surface tension and viscosity. However, the complex physics of dip-coating is not fully understood to develop theoretical models that can accurately predict the effect of surface tension and viscosity on coating uniformity and thickness, especially at the micron length scales of microneedles. Therefore, we dip-coated microneedles using different formulations to experimentally study their effect on coating uniformity and coating thickness.

First, microneedles were dipped in an aqueous solution containing sulforhodamine as a model drug. This formulation did not produce any coating on the microneedle (Fig. 3a). Thermodynamics of wetting dictates that only solutions that can completely wet the substrate i.e. have contact angles that approach zero can produce uniform films on the substrate, but the static contact angle of DI water on electropolished stainless steel was measured to be $47.5 \pm 3°$. This large contact angle is the result of the aqueous coating solution having a surface tension (72 mN/m at 25°C) (23) much larger than the stainless steel substrate (39.6 mJ/m^2) (24). We therefore added Lutrol F-68 NF, a surfactant, which lowered the coating solution surface tension and thereby decreased the

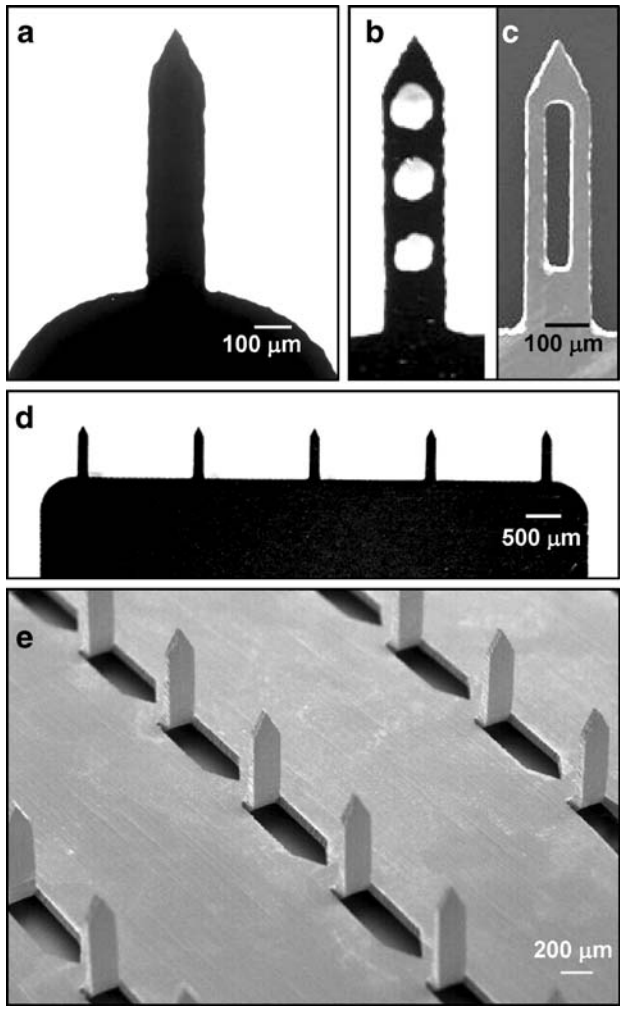

Fig. 1. The different microneedle designs used for coating experiments. Brightfield microscopy image of **a** a single microneedle and **b** a circular-pocketed microneedle. **c** Scanning electron microscopy image of a rectangular-pocketed microneedle. **d** Brightfield microscopy image of an 'in-plane' row of five microneedles attached to a macroscopic base substrate for ease of handling. **e** Scanning electron microscopy image of a section of an 'out-of-plane' array with 50 microneedles.

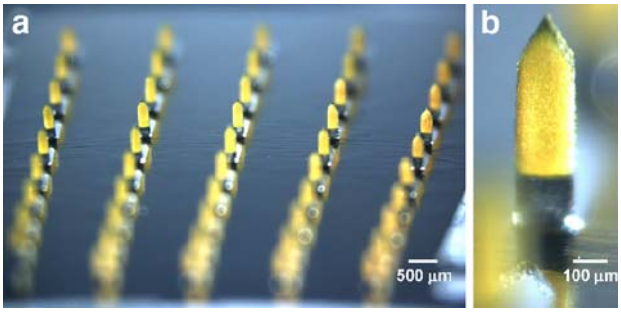

Fig. 2. Out-of-plane microneedle array uniformly coated with riboflavin. Imaging by brightfield microscopy shows **a** uniform coating of microneedle shafts without contamination of the base substrate of an array of 50 microneedles and **b** a representative magnified view of a single microneedle showing the uniform coating.

contact angle to 25.9 ± 5°. This produced a uniform, but thin, coating on the microneedles (Fig. 3b).

Thicker coatings should increase the drug loading on microneedles. Based on the hydrodynamics of dip-coating, thicker coatings can be obtained by increasing the coating solution viscosity, because elevated viscosity increases the hydrodynamic drag on the liquid during substrate withdrawal and leads to an increase in the volume of the liquid film that is formed on the microneedle upon withdrawal. Thus, to test the ability of a higher viscosity of the aqueous formulation to produce thicker coatings, CMC, a viscosity enhancer, was added to the aqueous coating solution. The surfactant, Lutrol F-68 NF was not included in the formulation to independently study the effect of the viscosity enhancer. Using a 1% (w/v) aqueous CMC solution (viscosity: 47 ± 0.5 mPa.s) as the coating solution, a thicker coating was produced on the microneedle. However, the coating was localized towards the center, away from the microneedle periphery (Fig. 3c). This phenomenon of de-wetting suggested that the high surface tension of the CMC-containing aqueous solution induced contraction of the liquid film on the microneedle during the drying phase.

Finally, we simultaneously modified the surface tension and the viscosity of the coating solution by adding both the surfactant and the viscosity enhancer, which resulted in thick and uniform coatings (Fig. 3d). Thus, application of the macro-scale principles of thermodynamics and hydrodynamics of wetting and dip-coating to the micron length scale of microneedles enabled the formation of (1) uniform coatings on microneedles by matching the surface energies of the coating solution and the substrate to promote wetting and (2) thicker coatings by increasing the viscosity of the coating solution, which increased the volume of the liquid film adhering to the microneedle upon withdrawal from the coating solution. These two criteria form a general basis for designing coating solution formulations to produce uniform coatings on microneedles.

In order to test the generality of these findings, we coated microneedles using another aqueous surfactant-viscosity enhancer system. Based on a previous study (17), we selected Tween 20 as the surfactant and sucrose as the viscosity enhancer. A similar trend in coating uniformity and thickness was observed for these aqueous coating solutions. A coating solution containing only Tween 20 (contact angle: 25.3 ± 4°) and sulforhodamine as the model drug resulted in a very thin, but uniform layer on the microneedle surface (Fig. 3e), while coating with only sucrose (52% w/w, viscosity: 18.7 ± 0.1 mPa.s) produced a thicker coating which was localized along the center of the microneedle shaft (Fig. 3f). Next, combining Tween 20 with sucrose increased the spread of the coatings on the microneedle surface, although the tip still remained uncoated (Fig. 3g). Thus, this surfactant-viscosity enhancer combination gave results similar to the Lutrol F-68 NF and CMC combination. Uncoated microneedle tips can slightly decrease the amount of drug coated onto microneedles. However, if this decrease is not significant, the excipients may be acceptable.

Choice of Excipients for Coatings

The previous set of experiments identified two formulations useful for microneedle coatings, both of which utilized excipients categorized by the FDA as safe for parenteral delivery (25). Optimization among these and other possible coating formulations will depend on drug physicochemical properties and needs of specific applications. For example, the use of CMC as a viscosity enhancer may be preferred over sucrose, because just 1% CMC (w/v) increased viscosity more than twice as much as 52% (w/w) sucrose. Minimizing excipient concentrations maximizes drug content in the coatings. Comparing the surfactants, Lutrol F-68 may be preferred over Tween 20, because Lutrol F-68, which is solid at room temperature, produced hard coatings, whereas, Tween 20, which is a liquid at room temperature, produced coatings with a waxy texture.

For specific applications, it may be desirable to use other excipients, for example, to avoid unfavorable drug-excipient interactions. Therefore, based on the coating formulation design criteria established above, we examined the ability of five additional viscosity enhancers in combination with Lutrol F-68 surfactant to produce good coatings. In all five cases, using hyaluronic acid (Fig. 3h), xanthan gum (Fig. 3i), sodium alginate (Fig. 3j), polyvinylpyrollidone (Fig. 3k) and sucrose (Fig. 3l) as the viscosity enhancers, thick uniform coatings were formed, although the sucrose formulations did not coat the tips, which may be due to the crystallinity and relatively high surface tension of sucrose. Altogether, this suggests that decreasing surface tension and increasing viscosity of the coating solution is a broadly applicable approach to rationally design optimized coating solution formulations.

Surface Modification for Coating

The addition of excipients may be undesirable for some drugs due to incompatibility between the drug and the excipients, which may lead to loss of drug activity (18). Rather than matching the surface energies of the coating solution and the microneedle surface by lowering the surface tension of the coating solution using a surfactant, we instead raised the surface energy of the stainless steel microneedles by making it more hydrophilic by pre-coating the microneedles with a thin layer of silicon dioxide. Subsequent coating with an excipient-free, aqueous solution of sulforhodamine resulted in a uniform but thin coating (Fig. 3m), consistent with coating using appropriately matched surface energies, but inadequate viscosity.

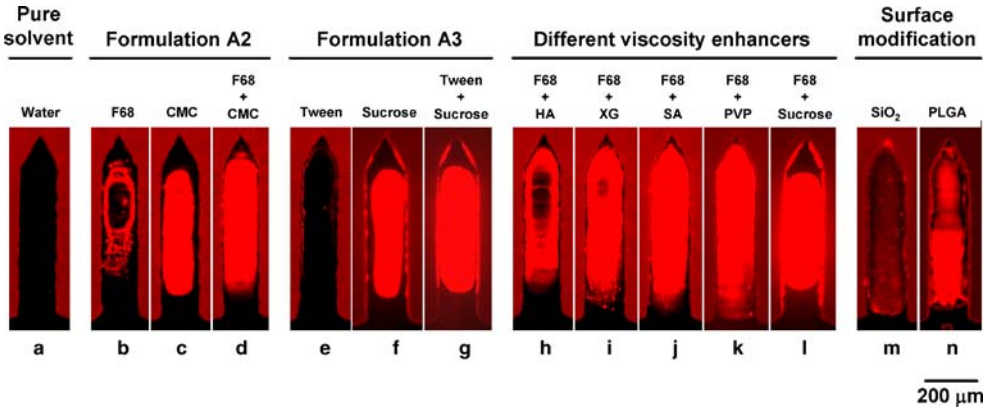

Fig. 3. Effect of surface tension and viscosity on coating uniformity on microneedles with sulforhodamine as the model drug. Fluorescence microscopy images with supplemental brightfield illumination to also view the microneedle outline after dip-coating single non-pocketed microneedles from different formulations. **a** Aqueous coating without excipients (Formulation A1). Based on Formulation A2, **b** coating only with Lutrol F-68 (F68), **c** coating only with carboxymethylcellulose (CMC), and **d** coating with the full formulation. Based on Formulation A3, **e** coating only with Tween 20, **f** coating only with sucrose, and **g** coating with the full formulation. Coating with F68 and **h** hyaluronic acid (HA) (Formulation A4), **i** xanthan gum (XG) (Formulation A5), **j** sodium alginate (SA) (Formulation A6), **k** polyvinylpyrrolidone (PVP) (Formulation A7), and **l** sucrose (Formulation A8). Aqueous coating without excipients (Formulation A1) on microneedle surfaces modified by pre-coating with **m** silicon dioxide (SiO_2) and **n** poly(lactic-co-glycolic acid) (PLGA).

As an additional approach, the stainless steel microneedle surface was pre-coated with PLGA, which also resulted in a uniform, but thin coating using an excipient-free solution (Fig. 3n). Although, PLGA provides a hydrophobic surface that does not improve the thermodynamics of the microneedle-coating solution surface energy mismatch, we believe it instead increased surface roughness, which increased the hydrodynamic drag to allow entrainment of a liquid film and reduced the surface tension-induced fluid contraction on the microneedle surface, and thereby increased the residence time for drying of a thin film on the PLGA surface. Although these excipient-free methods produced only thin coatings, surface modification may nonetheless be well suited for coating sensitive protein solutions, since protein solutions are often inherently viscous and can act as self-viscosity enhancers to increase the coating thickness.

Coating Proteins

To directly assess the ability of optimized formulations to coat proteins, we coated insulin and bovine serum albumin onto microneedles using Lutrol F68 as the surfactant and either CMC, hyaluronic acid or sodium alginate as the viscosity enhancer. Uniform coatings were obtained on the microneedle shafts for both proteins and all formulations tested (Fig. 4). These observations are consistent with our previous work (15), which demonstrated coating of peptides, proteins, DNA, viruses and microparticles. Together, these results suggest that the coating formulations developed in this study may have a broad applicability to coat a range of compounds and microparticles.

Coating Hydrophobic Molecules

Having studied a variety of approaches to coat microneedles from aqueous formulations, we next wanted to investigate coating of hydrophobic molecules. This provided an interesting formulation challenge, because excipients for this application need to be soluble in an organic coating solution solvent as well as soluble in the aqueous environment of the skin for rapid dissolution off the microneedle after insertion. We therefore selected an amphiphilic viscosity enhancer, polyvinylpyrrolidone (PVP), which has good solubility in water and in ethanol, the organic solvent selected for the coating solution. Use of an organic solvent also removed the need to add surfactant, since ethanol already has a low surface tension (21.8 mN/m at 25°C) (23). For this study, curcumin was used as the model hydrophobic drug. Curcumin is also fluorescent, making it easy to visualize the coatings.

Microneedles prepared using this formulation resulted in uniform coatings of the microneedle surfaces (Fig. 5a). Consistent with the design, dipping the coated microneedles into DI water for just 15 s completely removed the coatings. Even though curcumin has negligible solubility in water, dissolution of PVP excipient caused the microneedle coating to fall off the microneedle surface (Fig. 5b). Using an alternate approach, microneedles were coated using PLGA as the viscosity enhancer from an acetonitrile-based coating solution containing sulforhodamine. This formulation approach also resulted in uniform coatings (Fig. 5c). Because PLGA coatings degrade slowly in water, this formulation is envisioned to provide controlled release from coated microneedles left in the skin for an extended period of time.

Molten Coating Solutions

To simplify the coating formulation further, we next wanted to investigate coatings prepared without solvent or excipient. Because many solid drugs can remain stable above their melting point, microneedles could be coated by dipping them into pure drug as a molten liquid. This method would

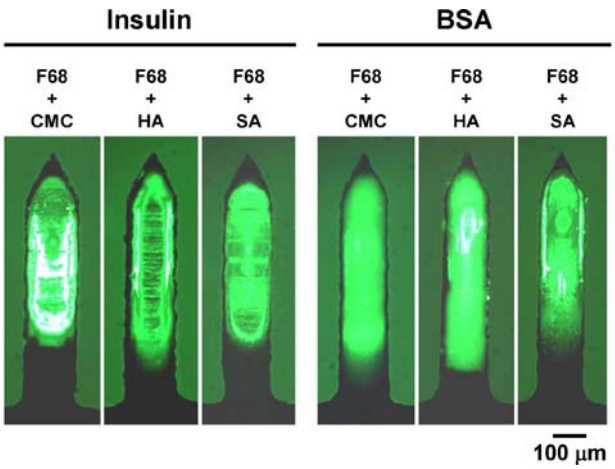

Fig. 4. Microneedles with protein coatings. Fluorescence microscopy images with supplemental brightfield illumination of single non-pocketed microneedles dip coated with fluorescein isothiocyanate-labeled insulin and bovine serum albumin (BSA) using Lutrol F-68 (F68) and carboxymethyl cellulose (CMC) (Formulation A2), Lutrol F-68 and hyaluronic acid (HA) (Formulation A4) and Lutrol F-68 and the sodium salt of alginic acid (SA) (Formulation A6).

enable coatings made of 100% drug and therefore result in higher mass loaded per microneedle. To test this idea, both pocketed and non-pocketed microneedles were dip-coated into molten lidocaine. Because the molten lidocaine was very viscous, the resulting coatings were thick and covered the entire surface in both non-pocketed (Fig. 5d) and pocketed (Fig. 5e) microneedles. As an additional model compound, molten polyethylene glycol (PEG) was coated onto microneedles, which was unable to coat non-pocketed microneedles well (data not shown). This probably occurred because molten PEG has high surface tension (45 mN/m at 70°C) (26). However, molten PEG was able to fill the interior of pocketed microneedles (Fig. 5f). These observations show that by using the molten liquid coating approach, drugs can be coated in their pure state on the surface of microneedles and inside microneedle pockets. As another variation, coating microneedles via the molten formulations may provide a way to coat and deliver hydrophobic molecules using molten polymers as a non-volatile solvent, because molten substances like PEG and PVP are known to improve solubility of hydrophobic drugs (27).

Pocketed Microneedles

We next wanted to explore other ways to fill drug formulations into microneedle pockets. Pockets in microneedles can provide a protective cavity that can be exploited to deliver drug formulations that would otherwise be difficult to coat onto microneedles or would wipe off on the skin surface during insertion. The previously successful formulation comprising Lutrol F-68 and CMC was used to coat pocketed microneedles, and was found to coat both the microneedle surfaces as well as fill the pockets (Fig. 5g). Thus, the use of formulations with surfactant and viscosity enhancer may provide a general method to coat and fill pocketed microneedles. However, in some circumstances it may be desirable to only fill the protective pockets without coating the microneedle surfaces. We were able to selectively fill the pockets by (1) removing the surfactant to inhibit surface wetting and increase the critical speed of liquid film formation, (2) keeping the viscosity enhancer to help retain coating solution within pockets, and (3) increasing the solids content by using 25% sucrose to help produce a conformal solid layer in the pockets (Fig. 5h).

In some cases it may be desirable to store and deliver a drug in liquid solution. Pocketed microneedles offer the further possibility to deliver drug formulations as liquids. In this way, the liquid can be protected from wiping off the microneedle during insertion into skin (see below). Dipping microneedles in a viscous glycerol solution containing sulforhodamine selectively filled the pockets without coating the microneedle surfaces (Fig. 5i). Glycerol has a high surface tension (62.5 mN/m at 25°C) (23) and such a high critical speed of liquid film formation that it does not produce liquid films on the microneedle surface. Yet, it is viscous enough to fill the pockets by counteracting the surface tension that tends to collapse the liquid drop formed inside the pocket. To further prevent micron-scale surface roughness from accumulating any liquid drops, microneedle withdrawal from the glycerol solution was done at a slow speed (about 0.35 mm/s). A limitation of this approach, however, is that the liquid in the pockets can evaporate: the glycerol in this example completely evaporated after approximately 24 h at ambient conditions. A similar coating using sulforhodamine dissolved in propylene glycol also selectively filled the pockets, but evaporated more rapidly (data not shown). For extended storage, these liquid filled pockets can be made more stable, for example, by packaging under pressure in a nitrogen atmosphere.

Composite Coatings

Some therapeutic delivery scenarios may require the application of different drugs from the same microneedle and may require different drug release profiles. To address this scenario, our next objective was to study composite drug coatings as a way to coat multiple drugs on the same microneedle. As a first example, microneedles were prepared to each have three circular pockets. Using the liquid glycerol method to selectively fill pockets, a sequence of dipping and washing steps (see "MATERIALS AND METHODS") was used to fill the upper pocket with a red dye, the middle pocket with a yellow dye and the lower pocket with a green dye (Fig. 5j). This "traffic signal" design enabled microneedles with three different model drugs each sequestered in different pockets to avoid drug–drug interactions.

We also explored ways to prepare layered coatings, such that each layer could contain different drugs and could be formulated to have different release kinetics. To have a burst release of a first drug followed by slow release of a second drug, a PLGA layer containing sulforhodamine was overcoated with water-soluble excipients containing sodium fluorescein (Fig. 5k). To achieve sequential burst releases separated by a delay, a coating made of water soluble excipients containing sulforhodamine was overcoated with PLGA followed by applying another layer containing water-soluble excipients and sodium fluorescein (Fig. 5l). As another double-burst approach, microneedle pockets were

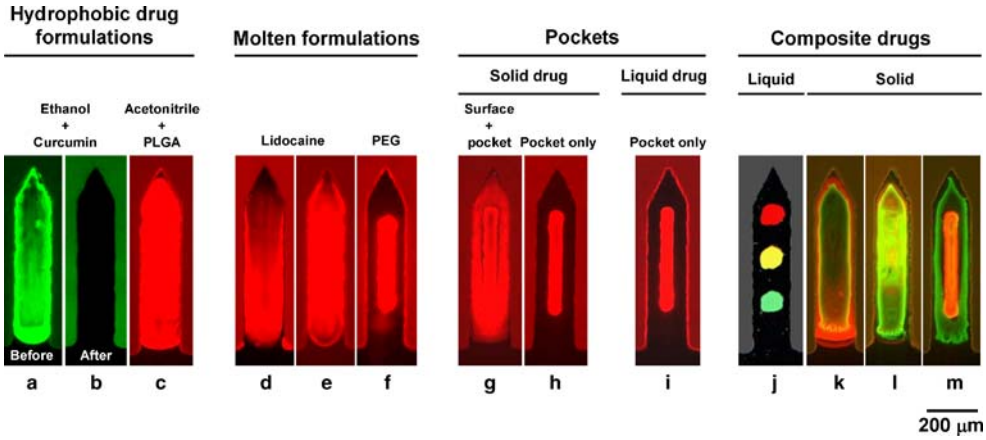

Fig. 5. Microneedles with hydrophobic coatings, molten formulation-based coatings, coatings of pocket designs, and composite coatings. Fluorescence microscopy images with supplemental brightfield illumination to also view the microneedle outline after dip coating single microneedles (non-pocketed unless specified) from different formulations. Coating resulting from Formulation O2, containing polyvinylpyrrolidone and fluorescent curcumin in ethanol solvent **a** before and **b** after dipping in water for dissolution test. **c** Coating resulting from Formulation O3, containing poly(lactic co-glycolic acid) (PLGA) in acetonitrile solvent with fluorescent sulforhodamine. Coating resulting from liquid molten lidocaine containing fluorescent sulforhodamine on **d** non-pocketed microneedles and **e** pocketed microneedles. **f** Coating resulting from liquid molten polyethylene glycol containing fluorescent sulforhodamine. Coatings of pocketed microneedle designs from aqueous solutions of fluorescent sulforhodamine, **g** using Formulation A2 containing carboxymethylcellulose and Lutrol F-68, **h** using Formulation A9 containing sucrose, and **i** using Formulation A10 containing glycerol. **j** Three circular pockets filled with glycerol solution containing a green dye (*bottom pocket*), a yellow dye (*middle pocket*) and a red dye (*apical pocket*) using Formulation A12, A13 and A14, respectively. **k** Two distinct coating layers from sequential dips, first in poly(lactic co-glycolic acid) (PLGA) in acetonitrile solvent with fluorescent sulforhodamine (Formulation O3) and then in an aqueous solution of carboxymethylcellulose, Lutrol F-68 and sodium fluorescein (Formulation A11). **l** Three distinct coating layers from sequential dips, first in an aqueous solution of carboxymethylcellulose, Lutrol F-68 and sulforhodamine (Formulation A2), then in poly(lactic-co-glycolic acid) in acetonitrile (Formulation O1) and lastly in an aqueous solution of carboxymethylcellulose, Lutrol F-68 and sodium fluorescein (Formulation A11). **m** Three distinct coating layers from sequential dips, first in an aqueous solution of sucrose containing fluorescent sulforhodamine (Formulation A9), then in poly(lactic-co-glycolic acid) in acetonitrile solvent (Formulation O1), and lastly in an aqueous solution of carboxymethylcellulose, Lutrol F-68 and sodium fluorescein (Formulation A11).

selectively filled with water-soluble excipients containing sulforhodamine and covered with PLGA, which was then followed by another layer containing water-soluble excipients and sodium fluorescein (Fig. 5m). Dipping these layered composite microneedles into DI water for 1 min caused the exposed water-soluble layers to dissolve, while the PLGA layers and the water-soluble layers beneath them remained intact (data not shown). Variations on these composite coatings could be tailored to meet drug delivery requirements for complex delivery profiles for single or multiple drugs.

Factors Affecting Mass in Coatings

Because microneedles are small, they are inherently limited to deliver small doses of drug. To determine how much drug could be delivered using microneedles and how to coat microneedles with controlled amounts of drug, we studied the effect of four parameters on the mass of drug coated onto microneedles using riboflavin (vitamin B_2) as the model drug. First, two coating parameters were examined, which showed that the concentration of drug in the coating solution and the number of coating dips increased both the mass of drug coated onto microneedles and the thickness of the coating (Figs. 6a and b). At the maximum concentration of riboflavin used (i.e. 4%), a mass of 2.6 ± 0.3 μg of riboflavin was coated per microneedle. At the maximum number of dips used (i.e. 24 dips), a mass of 6.4 ± 0.8 μg riboflavin was coated per microneedle. Although we determined that coatings containing up to 1.8 μg riboflavin (i.e. six dips) successfully inserted into porcine cadaver skin, thicker coatings may wipe off onto the skin surface during insertion, which would limit their utility. Despite this limitation, these results suggest that a patch about 10–20 cm^2 in size containing a few hundred microneedles is capable of delivering up to 1 mg of drug.

Changing microneedle design also affected drug coating. For example, increasing the number of microneedles from 5 to 50 did not change the drug mass on each microneedle and therefore proportionally increased the mass on the array approximately ten fold (Fig. 6c). This demonstrates the consistency and uniformity of the coatings among the needles of the arrays. Filling drug selectively into pockets reduced the amount of drug per microneedle. For example, filling the pockets with riboflavin using an aqueous formulation containing 3% riboflavin and 25% sucrose enabled loading up to 0.066 ± 0.013 μg per microneedle (Fig. 6d). Guided by these relationships, a single coating or microneedle parameter or a combination can be used to coat a pre-determined mass of drug onto microneedles.

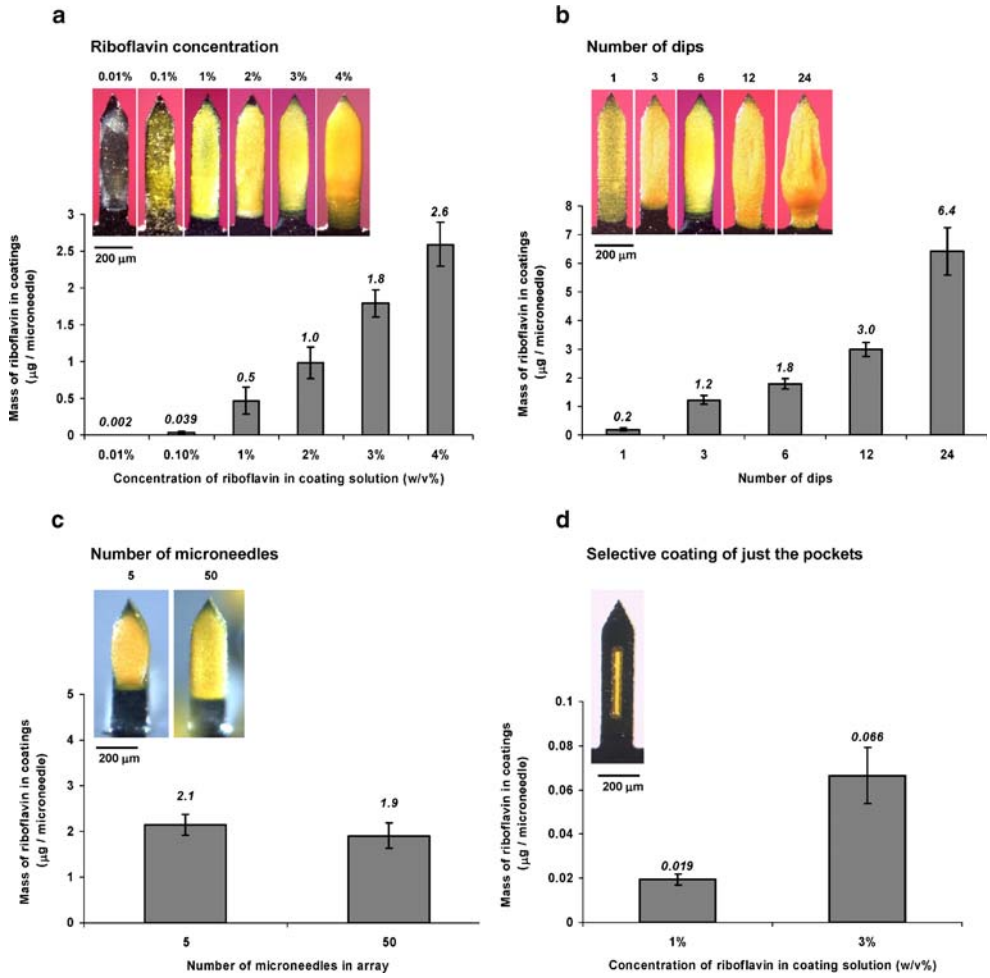

Fig. 6. Mass of riboflavin coated on microneedles as a function of formulation and microneedle parameters. Effect of **a** riboflavin concentration in coating solution, **b** number of coating solution dips, **c** number of microneedles in the array, and **d** riboflavin concentration during selective coating of microneedle pockets. The coatings were done using **a**, **b** and **c** Formulation A2, and **d** Formulation A9, with riboflavin as the model drug. Inset images show brightfield microscopy views of microneedles representative of the ones used to generate the data in the graphs.

As an additional assessment, we studied the reproducibility of controlling the amount of drug coated on to microneedles for drug delivery. While standard deviation bars are shown for the specific experiments in the graphs in Fig. 6, the average relative standard deviation (RSD) of all the standard deviation bars in Figs. 6a, b and c equals 19%. As a comparison, the 'readily acceptable' pass criteria established by the FDA for the manufacture of tablets and capsules is set at RSD $\leq$ 5% (28). We expect that since the current microneedle coating process is performed manually, improved control of temperature and humidity in the coating environment, precision in making coating formulations, and automation of the coating process should reduce the RSD to within acceptable limits.

In Vitro and *In Vivo* Insertion into Skin

It is important to prepare microneedle coatings that not only adhere to microneedles, but adhere to them during insertion into the skin and then dissolve off within the skin. To assess this, microneedles coated using many of the formulations discussed above were inserted into porcine cadaver skin. Coated microneedles were found to insert into the skin, their coatings did not wipe off onto the skin surface, and the coatings dissolved off the microneedles within less than 1 min and remained in the skin after microneedle removal.

Figure 7a shows a representative result for a non-pocketed microneedle coated with an aqueous formulation of sulforhodamine. The histological section of pig skin after insertion and removal of the microneedle displays the track left in the skin at the site of microneedle insertion and the fluorescence of coated sulforhodamine deposited in the skin. Note the lack of fluorescence on the skin surface consistent with deposition within the skin, and not on the surface. After removal, the microneedle was clean, indicating complete delivery of the coated formulation. No noticeable difference was perceived in the manual effort required to insert a coated versus an uncoated microneedle into porcine cadaver skin.

Through a companion study, quantitative assessment of the percentage of model drug delivered into the skin was made (15). It was found that after a 5-min insertion of riboflavin coated microneedle rows with five needle shafts,

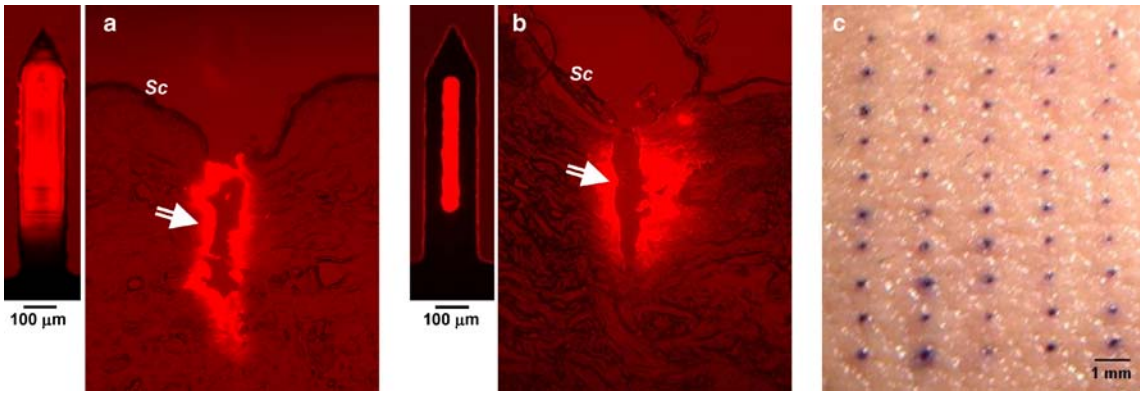

Fig. 7. Insertion of microneedles into skin *in vitro* and *in vivo*. Histological sections of porcine cadaver skin after insertion and removal of **a** a non-pocketed microneedle coated with a solid-phase (Formulation A2) and **b** a pocketed microneedle filled with a liquid-phase (Formulation A10). The images exhibit perforations in the skin at the sites of microneedle penetration, which are surrounded by fluorescence of sulforhodamine released from the coatings indicated by the *arrows*. *Images offset to the left* show the coated microneedles used at the same magnification. Imaging was done using combined brightfield and fluorescence microscopy. **c** Brightfield microscopy surface image of skin on the forearm of a human subject stained with gentian violet after insertion and removal of an out-of-plane, 50 microneedle patch. The sites of microneedle penetration into the skin are stained by the dye. Sc = Stratum Corneum.

91 ± 6% of the riboflavin was delivered into the skin, whereas 2 ± 1% was found on the skin surface and 7 ± 2% remained adhered to the microneedle surface after removal from the skin.

Figure 7b shows a representative result for a pocketed microneedle filled with a liquid, glycerol-based formulation of sulforhodamine. As proposed, the pocket protected and carried the liquid formulation into the skin for subsequent and rapid release within the skin. Microneedle insertion speed affected the tendency of the liquid in the coatings to wipe off on the skin surface. Low insertion speeds (0.5–1 mm/s), typically used for inserting microneedles coated with a solid film, led to wiping off of some liquid on the skin surface (data not shown). To prevent this liquid wipe off during insertion, higher insertion speed of about 1–2 cm/s was used, which reduced the contact time between the liquid contained in the pockets and the skin surface, thus preventing liquid wipe off on the skin surface.

As a final assessment, we wanted to determine if these microneedles can insert into the skin of human subjects *in vivo*. Because we did not have IRB approval to use coatings on human subjects, we inserted a non-coated 50-microneedle array into the skin of human subjects. After removing the microneedles, a dye was applied to the skin to stain the sites of microneedle penetration into the skin. Brightfield imaging of the skin surface displayed stained dots that correspond to the insertion sites of all 50 of the microneedles in the array (Fig. 7c). Insertion of 50-microneedle arrays into the skin of human subjects elicited mild sensation that was reported to be non-painful.

CONCLUSION

Motivated by previous demonstrations of peptide and protein delivery using coated microneedles, this study provides the first detailed examination of the design and control of microneedle coating formulations. First, stainless steel microneedles with or without pockets were fabricated by laser micromachining. Then, microneedle coating solution formulations were designed by recognizing the need to lower solution surface tension (1) to promote good wetting of the microneedle surface and (2) to decrease the critical speed of film formation, which facilitates retention of a liquid film on the microneedle after dipping. Good surface wetting was achieved through the addition of FDA approved surfactant excipients, the use of organic solvents, and modification of microneedle surface properties. Coating solutions were also designed to increase solution viscosity by using FDA approved viscosity enhancing excipients. Increased viscosity led to increased volume of liquid film adhering to the microneedles and an increased residence time of the adherent liquid film, producing thicker and more uniform coatings. When selectively filling pockets, increased solution viscosity was helpful, but surface tension was kept high in order to prevent coating of the microneedle surface.

Depending on drug properties, different aqueous, organic and molten coating formulations were used to coat microneedle surfaces and also to incorporate drugs into pockets in solid and liquid phases. Model proteins, insulin and bovine serum albumin, were coated onto microneedles using three different coating formulations, which demonstrates the versatility of this coating approach. Using an amphiphilic excipient, a hydrophobic molecule was also coated from an ethanol-based formulation and released from the microneedle in aqueous medium within 1 min. Composite drug coatings were applied as distinct layers, and to distinct regions on the microneedle, to either segregate different drugs from each other or to facilitate combination of burst and controlled release from the same microneedle.

The mass of a model drug, riboflavin, coated on microneedles was found to increase with its concentration in the coating solution, the number of coating solution dips, and the number of microneedles in the array. These data indicated that up to 1 mg of drug can be expected to be coated on a few hundred microneedles on a patch size of about 10–20 cm^2. The average relative standard deviation of the current microneedle coating process was found to be 19%, although reduced deviation is expected with automated manufacturing. Microneedle insertion into skin was demonstrated and shown to rapidly release coatings within the skin and not wipe off on

the skin surface. Altogether, this study shows that microneedle coating formulations can be designed to have a range of different properties to address a variety of different drug delivery scenarios.

ACKNOWLEDGMENT

We would like to thank Dr. Mark Allen for use of the IR and CO_2 lasers in his lab; Richard Shafer, Dr. Shawn Davis, and Ed Birdsell for helpful discussions regarding laser operation; and Dr. Jung-Hwan Park for making silicon dioxide coatings on microneedles. MRP is the Emerson-Lewis Faculty Fellow. This work was supported in part by the National Institutes of Health and took place in the Center for Drug Design, Development and Delivery and the Institute for Bioengineering and Bioscience at the Georgia Institute of Technology.

REFERENCES

1. M. R. Prausnitz, S. Mitragotri, and R. Langer. Current status and future potential of transdermal drug delivery. *Nat. Rev. Drug Discov.* **3**:115–124 (2004).
2. M. R. Prausnitz. Microneedles for transdermal drug delivery. *Adv. Drug Deliv. Rev.* **56**:581–587 (2004).
3. M. Prausnitz, J. Mikszta, and J. Raeder-Devens. Microneedles. In E. W. Smith and H. I. Maibach (eds.), *Percutaneous Penetration Enhancers*, CRC, Boca Raton, FL, 2005, pp. 239–255.
4. M. L. Reed and W.-K. Lyev. Microsystems for drug and gene delivery. *Proc. IEEE* **92**:56–75 (2004).
5. S. Henry, D. V. McAllister, M. G. Allen, and M. R. Prausnitz. Microfabricated microneedles: a novel approach to transdermal drug delivery. *J. Pharm. Sci.* **87**:922–925 (1998).
6. D. V. McAllister, P. M. Wang, S. P. Davis, J. H. Park, P. J. Canatella, M. G. Allen, and M. R. Prausnitz. Microfabricated needles for transdermal delivery of macromolecules and nanoparticles: fabrication methods and transport studies. *Proc. Natl. Acad. Sci. U. S. A.* **100**:13755–13760 (2003).
7. F. Chabri, K. Bouris, T. Jones, D. Barrow, A. Hann, C. Allender, K. Brain, and J. Birchall. Microfabricated silicon microneedles for nonviral cutaneous gene delivery. *Br. J. Dermatol.* **150**:869–877 (2004).
8. H. J. G. E. Gardeniers, R. Luttge, E. J. W. Berenschot, M. J. De Boer, S. Y. Yeshurun, M. Hefetz, R. Van't Oever, and A. Van Den Berg. Silicon micromachined hollow microneedles for transdermal liquid transport. *J. MEMS.* **12**:855–862 (2003).
9. R. K. Sivamani, B. Stoeber, G. C. Wu, H. Zhai, D. Liepmann, and H. Maibach. Clinical microneedle injection of methyl nicotinate: stratum corneum penetration. *Skin Res. Technol.* **11**:152–156 (2005).
10. W. Martanto, S. P. Davis, N. R. Holiday, J. Wang, H. S. Gill, and M. R. Prausnitz. Transdermal delivery of insulin using microneedles *in vivo*. *Pharm. Res.* **21**:947–952 (2004).
11. M. Cormier, B. Johnson, M. Ameri, K. Nyam, L. Libiran, D. D. Zhang, and P. Daddona. Transdermal delivery of desmopressin using a coated microneedle array patch system. *J. Control. Release* **97**:503–511 (2004).
12. J. A. Mikszta, J. B. Alarcon, J. M. Brittingham, D. E. Sutter, R. J. Pettis, and N. G. Harvey. Improved genetic immunization via micromechanical disruption of skin-barrier function and targeted epidermal delivery. *Nat. Med.* **8**:415–419 (2002).
13. W. Lin, M. Cormier, A. Samiee, A. Griffin, B. Johnson, C. L. Teng, G. E. Hardee, and P. E. Daddona. Transdermal delivery of antisense oligonucleotides with microprojection patch (Macroflux) technology. *Pharm. Res.* **18**:1789–1793 (2001).
14. J. A. Mikszta, V. J. Sullivan, C. Dean, A. M. Waterston, J. B. Alarcon, J. P. Dekker III, J. M. Brittingham, J. Huang, C. R. Hwang, M. Ferriter, G. Jiang, K. Mar, K. U. Saikh, B. G. Stiles, C. J. Roy, R. G. Ulrich, and N. G. Harvey. Protective immunization against inhalational anthrax: a comparison of minimally invasive delivery platforms. *J. Infect. Dis.* **191**:278–288 (2005).
15. H. S. Gill and M. R. Prausnitz. Coated microneedles for transdermal delivery. *J. Control. Release* **117**:227–237 (2007).
16. J. A. Matriano, M. Cormier, J. Johnson, W. A. Young, M. Buttery, K. Nyam, and P. E. Daddona. Macroflux microprojection array patch technology: a new and efficient approach for intracutaneous immunization. *Pharm. Res.* **19**:63–70 (2002).
17. G. Widera, J. Johnson, L. Kim, L. Libiran, K. Nyam, P. E. Daddona, and M. Cormier. Effect of delivery parameters on immunization to ovalbumin following intracutaneous administration by a coated microneedle array patch system. *Vaccine* **24**:1653–1664 (2006).
18. S. Yoshioka and V. J. Stella. *Stability of Drugs and Dosage Forms*, Kluwer, New York, 2002.
19. R. J. Stokes, D. F. Evans, and M. Errico. Liquid coating processes. In R. J. Stokes and D. F. Evans (eds.), *Fundamentals of Interfacial Engineering*, Wiley-VCH, Weinheim, Germany, 1997, pp. 399–456.
20. T. D. Blake and K. J. Ruschak. Wetting: static and dynamic contact lines. In S. F. Kistler and P. M. Schweizer (eds.), *Liquid Film Coating : Scientific Principles and Their Technological Implications*, Chapman & Hall, London, 1997, pp. 63–97.
21. L. E. Scriven. Physics and applications of dip coating and spin coating. In C. J. Brinker, D. E. Clark, and D. R. Ulrich (eds.), *Mat Res Soc Symp Proc*, Vol. 121, Materials Research Society, 1988, pp. 717–729.
22. H. S. Kheshgi. The fate of thin liquid films after coating. In S. F. Kistler and P. M. Schweizer (eds.), *Liquid Film Coating : Scientific Principles and Their Technological Implications*, Chapman & Hall, London, 1997, pp. 183–672.
23. D. R. Lide. *CRC Handbook of Chemistry and Physics,* 87th edition, CRC, Boca Raton, FL, 2006.
24. Q. Zhao, C. Wang, Y. Liu, and S. Wang. Bacterial adhesion on the metal-polymer composite coatings. *Int. J. Adhes. Adhes.* **27**:85–91 (2007).
25. A. H. Kibbe (ed.). *Handbook of Pharmaceutical Excipients*, American Pharmaceutical Association, Washington, D.C., 2000.
26. S. Cheboyina, J. O'Haver, and C.M. Wyandt. A mathematical model to predict the size of the pellets formed in freeze pelletization techniques: parameters affecting pellet size. *J. Pharm. Sci.* **95**:167–180 (2006).
27. C. Leuner and J. Dressman. Improving drug solubility for oral delivery using solid dispersions. *Eur. J. Pharm. Biopharm.* **50**:47–60 (2000).
28. *Draft Guidance for Industry on Powder Blends and Finished Dosage Units–Stratified In-Process Dosage Unit Sampling and Assessment*, Docket no. 2003D-0493, Federal Drug Adminstration, Rockville, MD, 2003.